JOURNAL OF GEOPHYSICAL RESEARCH, VOL. 112, C05048, doi:10.1029/2006JC004018, 2007

Tropical wave-induced oceanic eddies at Cabo Corrientes and the María Islands, Mexico

Luis Zamudio,[1] Harley E. Hurlburt,[2] E. Joseph Metzger,[2] and Charles E. Tilburg[3]

Received 14 November 2006; revised 8 February 2007; accepted 9 March 2007; published 30 May 2007.

[1] TOPEX/Poseidon and ERS-2 satellite altimeter observations and the 1/16° Naval Research Laboratory (NRL) Layered Ocean Model (NLOM) show the existence of anticyclonic eddies in the Cabo Corrientes – María Islands region off the Mexican West Coast. Analysis of the results demonstrates that: (1) The Cabo Corrientes - María Islands region is characterized by mean poleward coastal currents, driven by local wind forcing. (2) The local currents are intensified by the arrival of baroclinic downwelling coastally trapped waves (CTWs), generated in the equatorial Pacific. (3) Anticyclonic eddies are generated as the intensified local currents pass cape-like features in the coastline or shelf-break geometry. (4) From 1979 to 2001 the CTWs generated an average of 2.35 (2.5) Cabo Corrientes (María Islands) anticyclonic eddies per year. (5) The formation of eddies varies interannually, increasing (decreasing) during El Niño (La Niña) years. Comparison of a variety of numerical simulations, which include different dynamics and/or different wind forcing and/or different topographic effects, suggests that bottom topography, local wind, and baroclinic instabilities are not essential for the eddy generation. It is (a) the capes at Cabo Corrientes and the María Islands and (b) the strong transient events associated with the CTWs that are essential to the formation of these newly recognized eddies.

Citation: Zamudio, L., H. E. Hurlburt, E. J. Metzger, and C. E. Tilburg (2007), Tropical wave-induced oceanic eddies at Cabo Corrientes and the María Islands, Mexico, *J. Geophys. Res.*, *112*, C05048, doi:10.1029/2006JC004018.

1. Introduction

[2] Oceanic eddy formation due to the interaction of coastal currents with capes is a well documented process, which has been studied from several different points of view [*Røed*, 1980; *D'Asaro*, 1988; *Strub et al.*, 1991; *Klinger*, 1994a, 1994b; *Pichevin and Nof*, 1996; *Cenedese and Whitehead*, 2000; *Crawford et al.*, 2002; *Di Lorenzo et al.*, 2005]. The theories and observations presented in these studies have been used to explain the origin of the eddies observed near Cape St. Vincent (on the southwest coast of Portugal), Point Barrow (on the northeastern coast of Alaska), Capes Blanco and Mendocino (on the coasts of Oregon and California), and Cape St. James (on the southern tip of the Queen Charlotte Islands). However, so far as we are aware, no study has reported the existence and/or investigated the genesis of the oceanic eddies measured by satellite-altimeters near Cabo Corrientes and the María Islands (on the Mexican West Coast) (Figure 1).

[3] On the north side of Cabo Corrientes the bottom topography is characterized by an abrupt transition from a narrow to a wide shelf, while the coastline changes its orientation from SE-NW to approximately NS (Figure 2). North of Cabo Corrientes the María Islands Archipelago sits on a cape-like extension of the continental shelf (Figure 2). The mean surface ocean circulation at Cabo Corrientes and the María Islands is dominated by poleward coastal currents [*Zamudio et al.*, 2001]. The variability of the circulation near Cabo Corrientes and the María Islands is mainly dominated by equatorially generated (interannual and intraseasonal) and storm induced (higher frequency) coastally trapped waves (CTWs) [*Chelton and Davis*, 1982; *Christensen et al.*, 1983; *Enfield and Allen*, 1983; *Spillane et al.*, 1987; *Enfield*, 1987; *Merrifield and Winant*, 1989; *Merrifield*, 1992; *Kessler et al.*, 1995; *Ramp et al.*, 1997; *Zamudio et al.*, 2001, 2002, 2006].

[4] Results from numerical simulations, discussed herein, indicate that the mean poleward coastal currents at Cabo Corrientes and the María Islands are characterized by a speed of ~8 cm/s. However, the arrival of downwelling CTWs typically causes an increase to ~80 cm/s. The increased currents result in the formation of anticyclonic eddies. An eddy generation hypothesis based on the intensification of the local currents is presented and discussed in this study. The intensification of currents is produced by equatorially generated intraseasonal (30–90 days) and interannual (2–7 years) baroclinic downwelling CTWs. Intraseasonal downwelling Kelvin waves are a persistent characteristic of the boreal fall/winter season of the equatorial Pacific. The generation of these waves is increased

[1] Center for Ocean-Atmospheric Prediction Studies, Florida State University, Tallahassee, Florida, USA.
[2] Naval Research Laboratory, Stennis Space Center, Mississippi, USA.
[3] Department of Chemistry and Physics, University of New England, Biddeford, Maine, USA.

0148-0227/07/2006JC004018$09.00

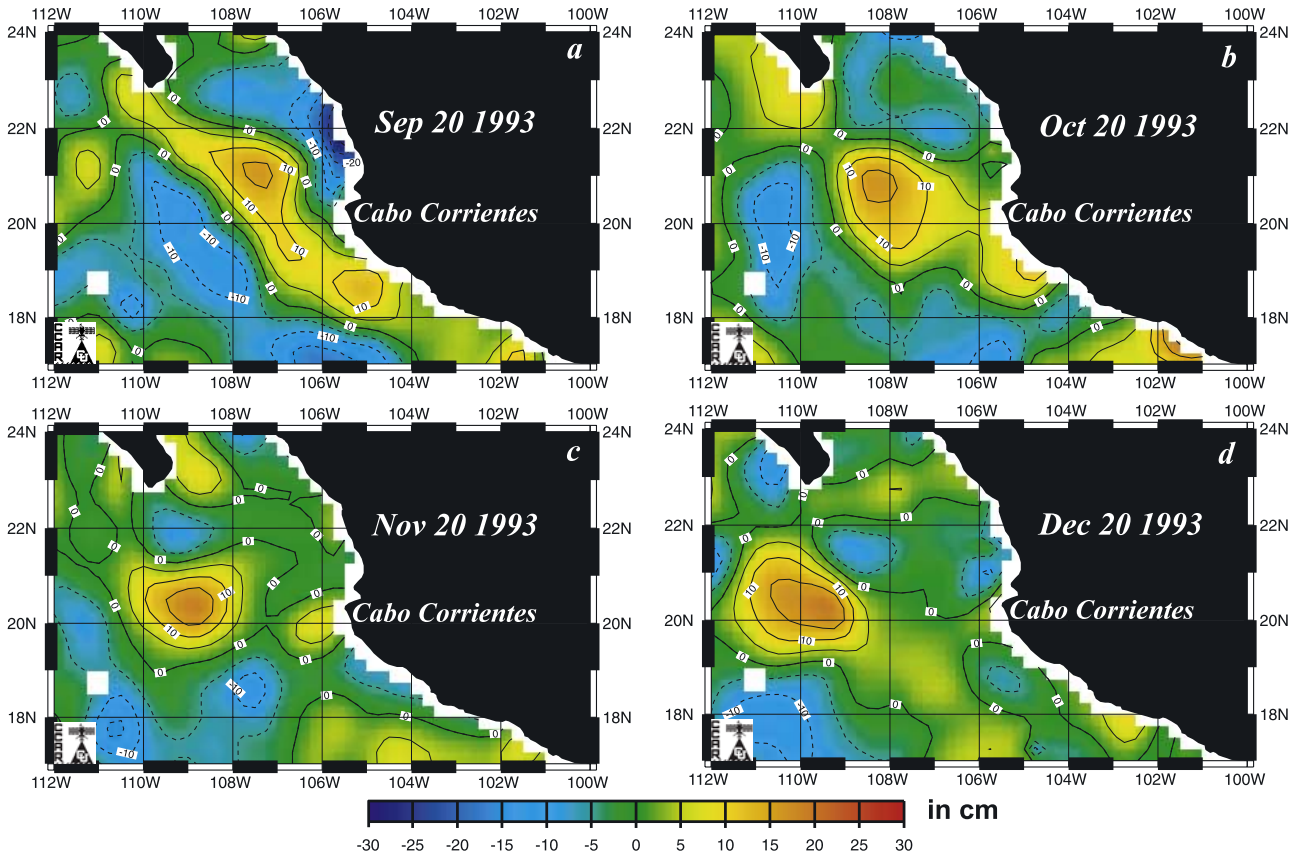

Figure 1. Sea surface height (SSH) anomaly (color contours in cm) for four different dates in 1993 as determined from TOPEX/ERS-2 satellite altimeters. These maps were designed to retain mesoscale sea surface height associated with fronts and eddies. They were obtained from the Colorado Center for Astrodynamics Research publicly accessible web site (http://www-ccar.colorado.edu/~realtime/global-historical_ssh).

during El Niño years; although, they are also evident during non–El Niño years [*Kessler et al.*, 1995]. These equatorial waves propagate eastward until they reach the eastern coastal boundary of the Pacific, where they split into northward and southward propagating CTWs with the northward CTWs reaching the Cabo Corrientes – María Islands region and far beyond [*Spillane et al.*, 1987; *Enfield*, 1987; *Kessler et al.*, 1995; *Meyers et al.*, 1998; *Melsom et al.*, 2003; *Zamudio et al.*, 2006].

[5] To determine the physical mechanisms responsible for the generation of these satellite detected eddies (Figure 1), a suite of numerical simulations is analysed where the dynamical complexity ranges from 1.5-layer reduced-gravity to 7-layer finite depth with realistic bottom topography. These are forced by five different wind products. The model results are compared with satellite altimeter measurements of sea surface height (SSH) and hydrographic data. Section 2 includes a description of the model and the experiments. Model results are presented and discussed in section 3. That section is divided in two subsections. The first one includes linear and nonlinear ocean model responses to monthly wind forcing, and nonlinear ocean model responses to 6-hourly wind forcing. The second subsection is devoted to the analysis of particular events. It includes examples of eddy formation during the passage of CTWs, the role of baroclinic instabilities, local wind, and bottom topography in the Cabo Corrientes - María Islands eddy generation, and a qualitative comparison between the observed and modeled eddies. Section 4 contains a summary and conclusions drawn from this research.

2. Model and Numerical Experiments

[6] The Naval Research Laboratory (NRL) Layered Ocean Model (NLOM) is a primitive equation layered formulation where the equations have been vertically integrated through each layer. It is a descendent of the model by *Hurlburt and Thompson* [1980]. Over the years it has been extensively augmented in capability [*Wallcraft*, 1991; *Wallcraft and Moore*, 1997; *Moore and Wallcraft*, 1998; *Wallcraft et al.*, 2003], applied to many research problems [*Hurlburt et al.*, 1996; *Metzger and Hurlburt*, 1996; *Shriver and Hurlburt*, 1997; *Hurlburt and Metzger*, 1998; *Hurlburt and Hogan*, 2000; *Metzger and Hurlburt*, 2001; *Zamudio et al.*, 2001; *Tilburg et al.*, 2001, 2002; *Hogan and Hurlburt*, 2000, 2005; *Melsom et al.*, 2003; *Kara et al.*, 2004; *López et al.*, 2005; *Zamudio et al.*, 2006], and it has been used for operational ocean prediction [*Rhodes et al.*, 2002; *Zamudio et al.*, 2002; *Smedstad et al.*, 2003; *Shriver et al.*, 2007]. The main features of the simulations used in this study are summarized in Table 1. Salient characteristics of NLOM are summarized below. Two differ-

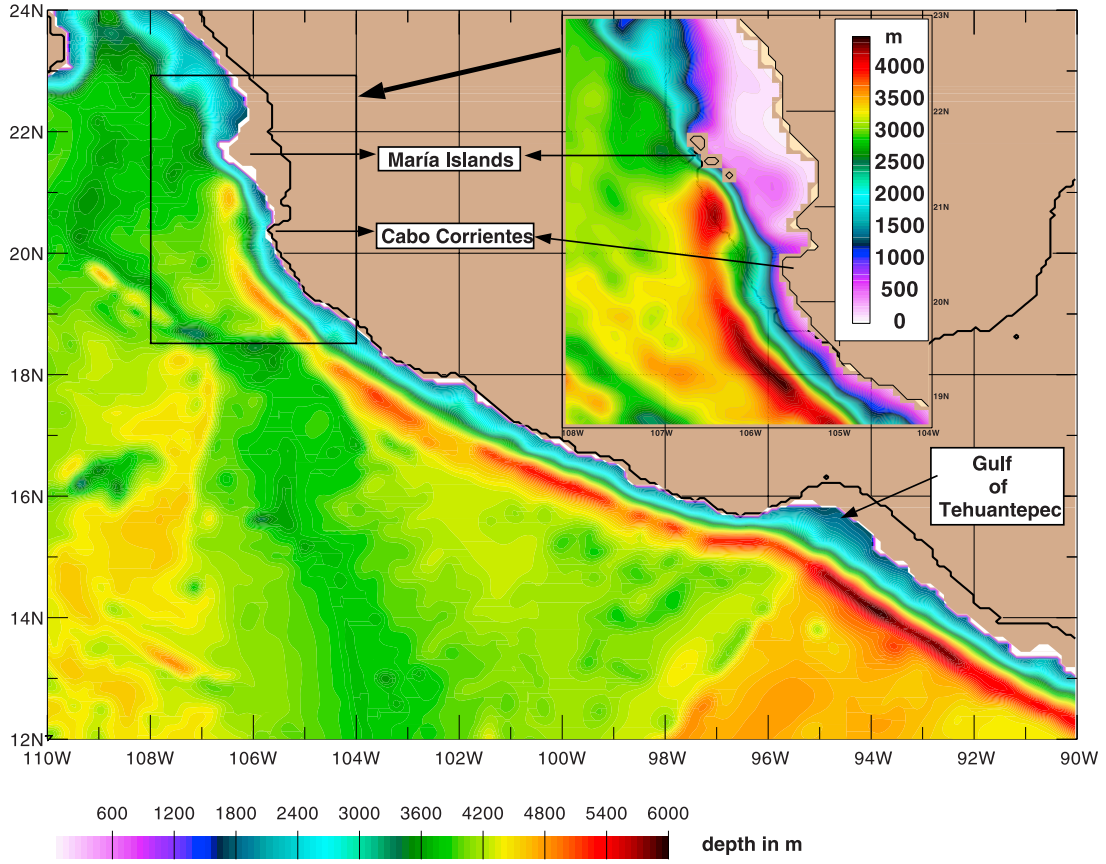

Figure 2. Model bottom topography (color) for the southwest coast of Mexico. Note the narrow shelf from west of the Gulf of Tehuantepec to Cabo Corrientes and how the María Islands lie on a cape-like extension of the continental shelf. The black continuous line represents the actual coastline.

ent model domains are used. The nearly global model domain extends from 72°S to 65°N, and the Pacific Ocean model domain extends from 20°S to 62°N and from 109.125°E to 77.2031°W, but here the focus is on the Cabo Corrientes - María Islands subregion (Figure 1). High-resolution (1/16° in latitude by 45/512° in longitude or ~8 km in the region of interest) is used for linear barotropic flat bottom and nonlinear model experiments. The model has a free surface and can be run in hydrodynamic mode or in thermodynamic mode with or without a mixed layer. Here the thermodynamic experiments include the mixed layer. The mixed layer implementation is discussed by *Wallcraft et al.* [2003]. The model experiments use 1, 1.5, 6 or 7 layers, realistic bottom topography, flat bottom or an infinitely deep bottom layer, and detailed coastline geometry. The bottom topography is a modified version of the 1/12° ETOPO5 [*National Oceanic and Atmospheric Administration*, 1986]. In most places the model geometry is determined by the 200 meter isobath,

Table 1. Summary of the Main Features of the Simulations Used in This Study[a]

Experiment	Linear (L)/ Nonlinear (NL)	A, m^2/s	Mean Layer Thicknesses, m	Period	Winds	Wind Frequency	Thermodynamic (T) Hydrodynamic (H)	Baroclinic Instabilities Allowed	Topographic Effects
PRG1.5ECH	NL	30	250/∞	1979–2000	ECMWF/HR	6 hours	H	No	No
PFB6ECH	NL	30	80/140/160/290/400/5430	1992–1999	ECMWF/HR	6 hours	H	Yes	No
PBT6ECH	NL	30	80/140/160/290/400/5430	1979–2000	ECMWF/HR	6 hours	H	Yes	Yes
PBT7ECH	NL	30	80/140/160/290/400/5430	1979–2001	ECMWF/HR	6 hours	T	Yes	Yes
PBT7NOH	NL	30	80/140/160/290/400/5430	1990–2001	NOGAPS/HR	6 hours	T	Yes	Yes
PBT7HRM	NL	30	80/140/160/290/400/5430	298–303	HR	Monthly	T	Yes	Yes
PBT7ECM	NL	30	80/140/160/290/375/5500	96–101	ECMWF	Monthly	T	Yes	Yes
GFB1HRM	L	30	250	1–3	HR	Monthly	H	No	No
GFB1ECM	L	30	250	1–7	ECMWF	Monthly	H	No	No
GFB1NOM	L	30	250	1–8	NOGAPS	Monthly	H	No	No

[a]Experiment naming convention is as follows. The first letter indicates the model domain: G for near global, and P for Pacific north of 20°S. The two letters that follow indicate model type: RG, reduced gravity; FB, flat bottom; and BT, realistic bottom topography. The number that follows indicates the number of layers used, including the mixed-layer in the thermodynamic simulations. The two letters that follow indicate the wind product used, HR for Hellerman and Rosenstein, EC for ECMWF, and NO for NOGAPS. The last letter indicates the frequency of the wind used to force the model: M for monthly, and H for 6-hourly. All the experiments included in this table have a resolution of 1/16° in latitude by 45/512° in longitude. "A" is coefficient of horizontal eddy viscosity.

which represents the nominal shelf break. Layer thicknesses and densities where chosen in accordance with the *Levitus and Boyer* [1994] and *Levitus et al.* [1994] climatologies.

[7] An important characteristic of the model is isopycnal outcropping that is incorporated by entrainment from the layer below whenever a layer becomes thinner than a prescribed minimum layer thickness. Volume is conserved within the layers such that entrainment in one layer is balanced by an equal amount of detrainment elsewhere in the model domain [*Shriver and Hurlburt*, 1997]. The model boundary conditions are kinematic and no slip. The latitudinal extent of the model domains (72°S–65°N, and 20°S–62°N) allows equatorially generated signals (i.e., CTWs) to influence the circulation of the eastern North Pacific Ocean, including the Cabo Corrientes - María Islands region.

[8] Wind stress is the key external forcing in the simulations reported here, although thermal forcing is included in the thermodynamic experiments. As a first step, linear 1/16° barotropic flat bottom simulations were performed using *Hellerman and Rosenstein* [1983] (HR), European Centre for Medium-Range Weather Forecasts (ECMWF) [*ECMWF*, 1994], and Fleet Numerical Meteorology and Oceanography Center Navy Operational Global Atmospheric Prediction System (NOGAPS) [*Rosmond et al.*, 2002] wind stress climatologies (Table 1). Since the linear simulations reveal the lowest order ocean response to the wind forcing, they are used as a baseline to help interpret the more complicated simulations that incorporate nonlinearities, bottom topography, multiple vertical modes, and flow instabilities (Table 1). The nonlinear climatological 1/16° simulations were spun up to statistical equilibrium first at 1/8°, then continued at 1/16° resolution using the same (HR or ECMWF) monthly wind stress climatology. The interannual simulations were initialized from the corresponding climatological HR simulation (some not listed in Table 1), then forced by 6-hourly ECMWF or NOGAPS winds and thermal forcing. The ECMWF or NOGAPS long-term temporal mean, was replaced by the annual mean from HR to produce a hybrid wind set (ECMWF/HR or NOGAPS/HR). As reported by *Metzger et al.* [1992], a more realistic mean state could be obtained in the ocean model by using the hybrid wind set. The linear simulations forced by the different wind climatologies assisted in verifying that HR is a good choice for the long-term mean wind stress. Using the hybrid winds, the long-term mean solution is driven primarily by the HR climatology, but intraseasonal, seasonal, and interannual forcing is from ECMWF or NOGAPS. The hybrid winds also reduce spurious spin-up effects at the beginning of the interannual simulations initialized from HR. In addition to the wind forcing, the four thermodynamic simulations (Table 1) were forced with daily average heat fluxes from ECMWF using model sea surface temperature (SST) in the calculation of latent and sensible heat flux via the bulk formulae of *Kara et al.* [2002]. The Kara et al. formulation was also used to convert ECMWF 10 m winds to surface stresses, but NOGAPS surface stresses were used for NOGAPS-forced simulations.

[9] Isolating the physical processes that contribute to the formation of the Cabo Corrientes and María Islands eddies is the particular focus of this study. Because the local wind stress curl is a potential eddy generator, local accuracy in the model wind forcing is essential. However, CTWs of equatorial origin are critical in eddy generation near the Cabo Corrientes and María Islands. Hence, accurate HR, ECMWF, and NOGAPS winds over the equatorial Pacific are also essential.

3. Results and Discussion

[10] In this section NLOM long-term means and snapshots are described and analyzed. Considering that the model results include several thousand snapshots, the instantaneous oceanic features are presented and discussed using an illustrative example. The example represents the five simulations forced with 6-hourly winds (Table 1) and corresponds to eddy formation during 1992. The year 1992 was selected because all the simulations forced with high frequency winds, which are discussed in this study, include results for that year (Table 1), and (more importantly) because the hydrographic data that are used to validate the model results are only available for a short period of time during 1992.

3.1. Long-Term Mean

3.1.1. Oceanic Response to Monthly Wind Forcing

[11] The wind stress and wind stress curl from ECMWF and HR at Cabo Corrientes and the María Islands are dominated by a curl dipole that is characterized by a region of negative curl on the offshore side and positive curl on the onshore side (Figures 3a and 3b). The positive curl extends along the coast from the entrance of the Gulf of California (24°N) to ~17°N and includes along the coast maxima to the north and south of the María Islands (Figures 3a and 3b). These two wind products also feature a weak upwelling favorable wind. Using a SeaWinds satellite scatterometer wind set, *Kessler* [2002] reported one year mean (August 1999 – July 2000) wind stress and wind stress curl fields which show upwelling favorable winds and near shore positive wind stress curl as in the ECMWF and HR winds (Figures 3a and 3b). Thus, there is a qualitative concordance between the ECMWF and HR annual mean wind sets and the measurements (and calculations) of the satellite-scatterometer wind set in this region (see Figure 5 from *Kessler* [2002]). In contrast, the NOGAPS annual mean wind set differs from the satellite scatterometer results (Figure 3c). NOGAPS wind stress does not include the upwelling favorable winds along mainland Mexico and also shows areas of negative wind stress curl along the coast (Figure 3c).

[12] The mean local currents along Cabo Corrientes and the María Islands from the three linear barotropic flat bottom simulations consist of a coastal or near coastal poleward flow of ~2 cm/s extending ~200 km offshore (Figures 4a–4c). These eastern boundary currents are the lowest order flat bottom ocean model response to the local wind stress curl (Figure 3), local because of the proximity to the eastern boundary. The existence of these currents is explained by the *Sverdrup* [1947] balance. The meridional transport/unit width in MKS units of m^2/s is given by $\beta V = curl\,(\tau)$, where the vertically integrated meridional transport/unit width (β), which is converted to depth-averaged currents in Figure 4, is a function of the local wind stress curl (τ) (Figure 3), and β, the meridional rate of change of the Coriolis parameter. Hence, in accordance with Sverdrup

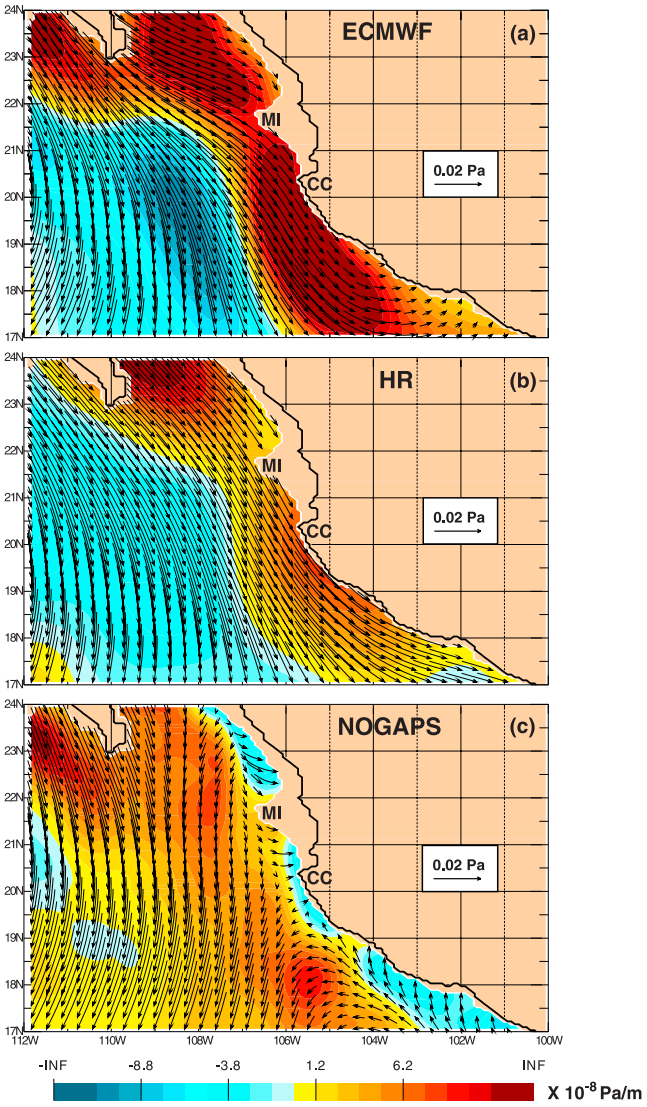

Figure 3. Wind stress (arrow vectors) and wind stress curl (color contours in 1×10^{-8} Pa/m) from long-term mean climatologies (a) European Centre for Medium-Range Weather Forecasts (ECMWF) [*ECMWF*, 1994], (b) *Hellerman and Rosenstein* [1983] (HR), (c) Fleet Numerical Meteorology and Oceanography Center's Navy Operational Global Atmospheric Prediction System (NOGAPS) [*Rosmond et al.*, 2002]. The positions of Cabo Corrientes (CC), and the María Islands (MI) are indicated.

balance, the alongshore positive wind stress curl generates poleward currents (Figures 3 and 4). The currents round both Cabo Corrientes and the María Islands remaining adjacent to the coast (Figures 4a and 4b). There is no evidence of mean coastal eddies in the simulations forced with ECMWF and HR winds (Figures 4a and 4b), but the simulation forced with NOGAPS wind stress (Figure 4c) includes closed circulations adjacent to the coast that are consistent with the areas of alongshore negative wind stress curl (Figure 3c). How do nonlinear processes modify the coastal poleward currents of the region?

[13] The two nonlinear simulations forced with climatological monthly winds (PBT7HRM, and PBT7ECM in Table 1) show the poleward surface currents in the vicinity of Cabo Corrientes and the María Islands (Figure 5). The surface currents are stronger (~8 cm/s) and narrower (offshore extension of ~60 km) than the linear barotropic

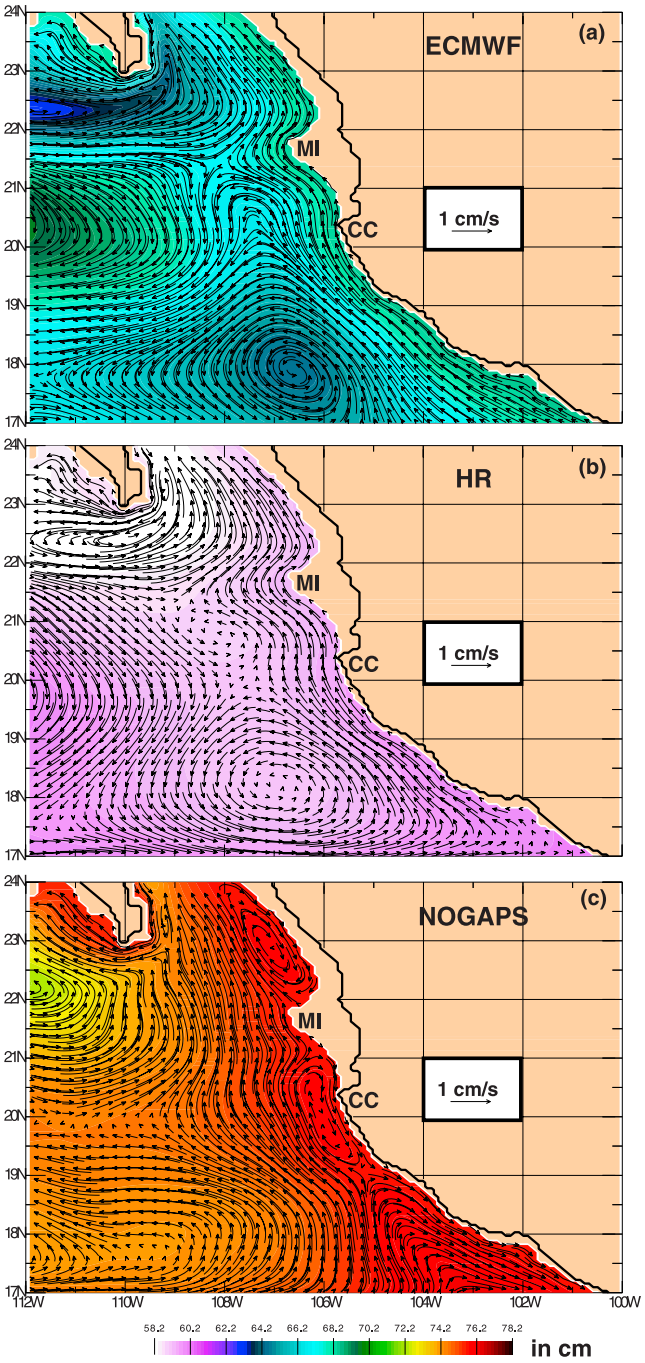

Figure 4. Long term mean SSH (color) and depth-averaged currents (arrow vectors) as determined from a global linear, barotropic, flat bottom configuration of the Naval Research Laboratory (NRL) Layered Ocean Model (NLOM), which was forced with the three different wind products shown in Figure 3. Model forced with: (a) ECMWF (exp. GFB1ECM), (b) HR (exp. GFB1HRM), (c) NOGAPS (exp. GFB1NOM). The positions of Cabo Corrientes (CC), and the María Islands (MI) are indicated.

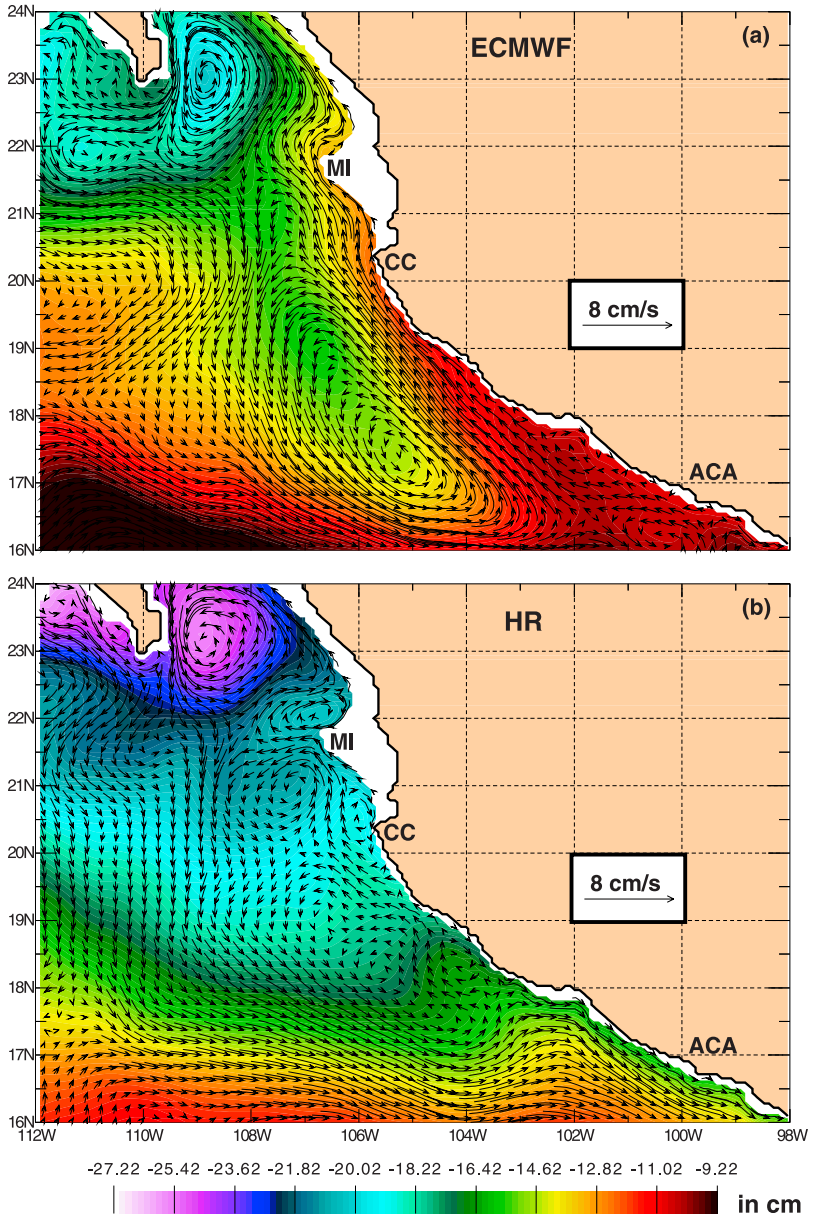

Figure 5. Long term mean sea surface height (color) and surface currents (arrow vectors) as determined from a Pacific Ocean 7-layer nonlinear thermodynamic configuration of NLOM with a mixed layer, which was forced with: (a) ECMWF (exp. PBT7ECM), and (b) HR (exp. PBT7HRM) from Figure 3. The positions of Cabo Corrientes (CC), María Islands (MI) and Acapulco (ACA) are indicated.

currents (Figure 4). Also, there are some differences between the two simulations in Figure 5. For instance, in the simulation forced with HR winds the currents around the Cabo Corrientes - María Islands region are weaker than the currents in the simulation forced with ECMWF winds. Furthermore, the simulation forced with HR winds includes mean anticyclonic (cyclonic) circulation to the north (south) of the María Islands, which is barely evident in the simulation forced with ECMWF winds.

[14] Overall, both linear and nonlinear simulations include the mean near-coastal poleward currents, which are basically the ocean response to the local nearshore positive wind stress curl (Figure 3), extending from northwest of the Acapulco region to the mouth of the Gulf of California (Figures 4 and 5). *Badan-Dangon et al.* [1989] and *Badan-Dangon* [1998] invoked on the existence of poleward coastal currents in the region, which the authors named the Mexican Current. However, to the best of our knowledge, the only two pieces of evidence for the existence of these mean poleward coastal currents, reported in the literature, are (1) model results from NLOM (see Figure 1b from *Zamudio et al.* [2001]), which were recently validated by (2) the direct observations of Lavin et al. [2006]. Now, Figures 3–5 demonstrate the locally forced nature of the coastal feature, the Mexican Current.

3.1.2. Ocean Model Response to Six-Hourly Wind Forcing

[15] In the context of this study the most significant difference between the results of the nonlinear simulations forced with monthly and six-hourly winds is the formation of

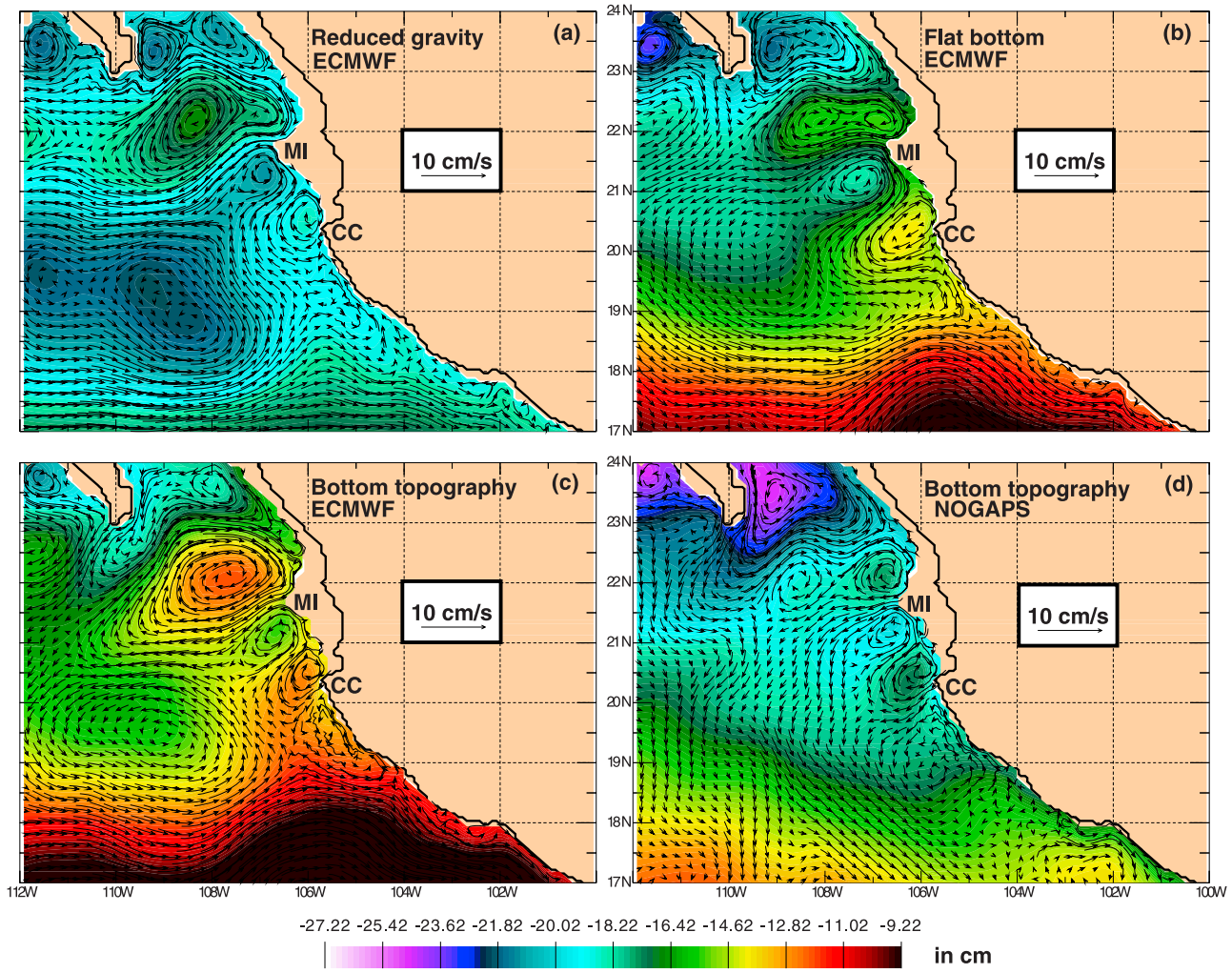

Figure 6. Eight year mean (1992–1999) SSH (color) and surface currents (arrow vectors) as determined from different configurations of NLOM, which were forced with 6-hourly winds: (a) 1.5-layer, reduced-gravity forced with ECMWF/HR winds (experiment PRG1.5ECH), (b) 6-layer, flat-bottom forced with ECMWF/HR winds (experiment PFB6ECH), (c) 7-layer, bottom topography forced with ECMWF/HR winds (experiment PBT7ECH), (d) 7-layer, bottom topography forced with NOGAPS/HR winds (experiment PBT7NOH). The positions of Cabo Corrientes (CC) and María Islands (MI) are indicated.

much stronger mean anticyclonic eddies northwest of Cabo Corrientes and the María Islands in the simulations forced with six-hourly winds (Figure 5 versus Figure 6). These anticyclonic eddies are revealed as two independent coastal structures with maximum SSH at the center of each eddy (Figure 6). The two eddies are basically in the same location, in the four different simulations in Figure 6, and they show up as distinctive coastal signals, suggesting a coastal geographical formation mechanism, which could be permanent or appear frequently enough to generate a large number of eddies, which have an impact in the 8-year means (1992 to 1999) in Figure 6.

[16] The two nonlinear simulations forced with climatological monthly winds at most include only weak mean anticyclonic eddies in the Cabo Corrientes - María Islands region (Figure 5). This is an expected result since the central hypothesis of this research postulates intraseasonal (30–90 days), and interannual (2–7 years) equatorially generated CTWs as the main forcing of these eddies, and waves in the intraseasonal frequency band can not be generated by climatological monthly winds. Consequently, the two simulations in Figure 5 only include CTWs driven by the mean seasonal cycle. However, the influence of those waves in the Cabo Corrientes - María Islands eddy generation is not enough to strongly impact in the mean fields in these simulations. Conversely, the six-hourly winds can generate intraseasonal baroclinic equatorial Kelvin waves, which propagate eastward until they reach the eastern boundary coast, where they split into northward and southward propagating CTWs with the northward CTW reaching the Cabo Corrientes and María Islands region [*Spillane et al.*, 1987; *Enfield*, 1987; *Kessler et al.*, 1995]. The ability of NLOM to simulate intraseasonal CTWs propagating along the coast of the Eastern Pacific has already been extensively documented [*Meyers et al.*, 1998; *Melsom et al.*, 1999; *Murray et al.*, 2001; *Zamudio et al.*, 2001; *Melsom et al.*,

2003; *López et al.*, 2005; *Zamudio et al.*, 2006]. How do intraseasonal baroclinic CTWs influence on the generation of the Cabo Corrientes and María Islands eddies? Why do the local coastal-attached poleward currents not generate eddies at Cabo Corrientes – María Islands by themselves?

[17] The processes of eddy formation at capes have already been investigated using the assumption of a steady coastal current. A detailed description of those processes can be found in the work of *Bormans and Garret* [1989], *Pichevin and Nof* [1996], and references therein. The more relevant features are summarized below. Consider a steady coastal current that encounters a cape and rounds it to continue its advance as a boundary current. If the radius of curvature of the cape is smaller than the inertial radius ($|\vec{u}|/f$, where $|\vec{u}|$ is the characteristic speed of the current in question, and f is the Coriolis parameter) the current will separate from the coast [*Bormans and Garret*, 1989; *Hughes*, 1989; *Klinger*, 1994a, 1994b]. After separation the current must reattach to the coast due to its finite offshore extension, which is proportional to the radius of deformation [*Bormans and Garret*, 1989]. The separation and reattachment of the current produces a dynamically unbalanced flow around the cape that is rebalanced via the formation and shedding of eddies [*Pichevin and Nof*, 1996].

[18] For Cabo Corrientes and the María Islands the model radii of curvature are ~12 km and ~10 km, respectively. However, the model poleward mean currents with $|\vec{u}| = 8$ cm/s (Figure 6), and $f = 5 \times 10^{-5}$ have an inertial radius of only ~1.6 km, and consequently the mean currents do not separate from the capes. In contrast, the downwelling CTWs increase the currents to $|\vec{u}| > 80$ cm/s (section 3.2), resulting in currents with an inertial radius >16 km, which is larger than the model radii of curvature of Cabo Corrientes and the María Islands. Therefore, the reinforced currents may separate from the coast at Cabo Corrientes and the María Islands, and form eddies (e.g., Figure 6 and section 3.2). Thus, in the Cabo Corrientes – María Islands scenario the eddy forcing is not a steady forcing but an intermittent forcing that appears with the arrival of CTWs. Cabo Corrientes means ''cape of currents'', a name choice possibly influenced by the strong intermittent currents produced by the CTWs.

[19] There are several salient features of the simulations in Figure 6. All the simulations forced with six-hourly winds (ECMWF or NOGAPS, bottom topography or flat bottom or reduced-gravity) generated the Cabo Corrientes and María Islands eddies. The 1.5-layer reduced-gravity simulation generates strong anticyclonic Cabo Corrientes and María Islands eddies, which are located to the northwest of the corresponding eddies in the rest of the simulations in Figure 6. The vertical resolution has a critical impact on the strength and northwest path of these eddies. In a 1.5-layer reduced-gravity simulation the eddies can not pump energy to any other vertical mode as in the other more dynamically complex simulations (e.g., 6 and 7 layer simulations (Figures 6b–6d)). Thus, the anticyclonic eddies feature a larger downward isopycnal displacement at the core. This core propagates to the west faster than the edge of the eddies, producing stronger currents on the west side of the eddies and northwestward self-advection/propagation of the eddies, as discussed by *Smith and Bird* [1989].

[20] The María Islands generate a stronger mean eddy than Cabo Corrientes (Figure 6). The María Islands sharp cape could be a critical factor in the formation of strong eddies. To understand this, it is important to remember that the model uses the continental shelf break (200 meter isobath) as a land-sea boundary. Since depths between the María Islands and the continent are mostly shallower than 200 meters, the María Islands can be visualized as an extension of the continental shelf forming a sharper María Islands' cape in the model than Cabo Corrientes (Figure 2). Furthermore, since the continental shelf break is the waveguide for CTWs the model land-sea boundary is appropriate for the propagation of CTWs, although, it limits the development of continental shelf waves and the incorporation of coastal barotropic dynamics.

[21] The CTWs discussed in this study are generated by wind-driven intraseasonal equatorial Kelvin waves. Thus, the intraseasonal CTWs arriving in the Cabo Corrientes – María Islands region are surface-intensified and they generate the surface-intensified Cabo Corrientes and María Islands eddies. However, even with their surface-intensified genesis, these eddies are a coherent signal from the surface to the bottom of the ocean (Figure 7). Note how in the simulation including realistic bottom topography (Figures 7a–7c) the abyssal currents are well established and follow the f/h contours (Figures 7c and 2), where f is the Coriolis parameter and h is the depth of the water column. In contrast, in the simulation with a flat bottom (Figures 7d–7f) the abyssal currents are extremely weak.

3.2. Synoptic Events Near Cabo Corrientes and the María Islands

[22] This subsection is divided into three parts. First, a sequence of snapshots from simulation PBT7ECH is used in describing and analyzing mesoscale eddy generation near Cabo Corrientes and the María Islands in association with the arrival of CTWs. Second, the eddy generation processes are discussed, and finally model results are compared with observations.

3.2.1. Coastally Trapped Waves and Eddy Formation

[23] Before the arrival of the downwelling CTW in the Cabo Corrientes - María Islands region the SSH anomaly is small (<10 cm) (Figure 8a), the thermocline depth is ~60 m (not shown), the current speed is ~25 cm/s (not shown), and no coastal eddy activity can be recognized in the area. Later, upon the arrival of a downwelling CTW the SSH anomaly, thermocline depth and current speed increase to ~20 cm (Figures 8b–8d), ~90 m (not shown), and ~70 cm/s (not shown), respectively. In addition, anticyclonic eddy formation can be recognized on the northern sides of the Cabo Corrientes and María Islands capes (Figures 8b–8d). The eddy formation continues (Figures 8d–8f) and by February 3, 1992 eddies have formed downstream of the capes (Figure 8g). Some days later the entire CTW has crossed the region and the Cabo Corrientes and María Islands anticyclonic eddies detach from the coast and propagate southwestward at 7.2 and 5.2 cm/s, respectively (Figures 8h–8l).

[24] Some salient points concerning the generation of these eddies are: (1) The eddy formation process took around 15 days from the time the CTW arrived in the area

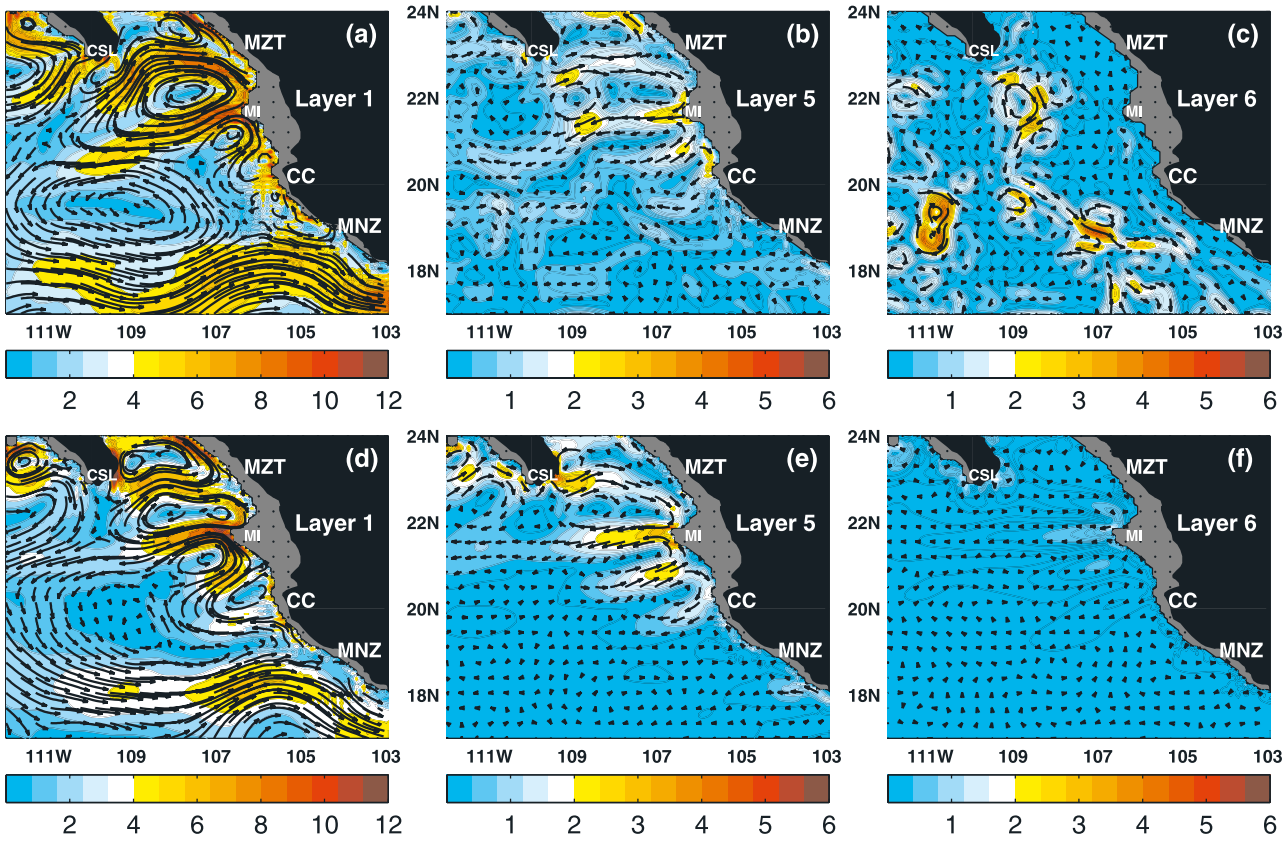

Figure 7. Mean currents (arrow vectors) and current speed (color contours in cm/s) for the period 1992–1999 for three dynamical layers as determined from (a–c) experiment PBT7ECH and (d–f) experiment PFB7ECH. The positions of Manzanillo (MNZ), Cabo Corrientes (CC), María Islands (MI), Mazatlán (MZT), and Cabo San Lucas (CSL) are indicated.

on January 19, 1992 (Figure 8b) until the two eddies were completely formed on February 3, 1992 (Figure 8g). (2) The same CTW generated a third anticyclonic eddy near Cabo San Lucas (on the southern tip of the Baja California Peninsula) (Figures 8a–8l). (3) On February 15, 1992 the Cabo Corrientes (María Islands) eddy was characterized by a radius (radius of the maximum swirl velocity) and swirl velocity of ~41 (28) km, and ~30 (60) cm/s, respectively (Figure 8i).

[25] On February 24, 1992 an upwelling CTW arrived in the area (Figure 8j). The Cabo Corrientes and María Islands anticyclonic eddies weakened (Figures 8i–8m), and the upwelling CTW generated a cyclonic eddy on the southern side of the María Islands (Figure 8m). However, some days later a strong downwelling CTW arrived in the region affecting the existing María Islands eddies, and largely damping the cyclonic eddy and totally absorbing the anticyclonic eddy (Figures 8m–8o). Consequently, on March 14, 1992 the anticyclonic Cabo Corrientes and Cabo San Lucas eddies were the only two active eddies in the region (Figure 8o). The strong downwelling CTW generated a SSH anomaly of >25 cm (Figure 8o) and current speeds >90 cm/s. On March 20, 1992 anticyclonic eddy formation occurred NW of both capes (Figure 8p). This CTW generated three new anticyclonic eddies, including one off Cabo San Lucas (Figure 8s). During the first week of April 1992, two Cabo San Lucas, two Cabo Corrientes and one María Islands anticyclonic eddies can be observed in the area (Figures 8s and 8t).

[26] In contrast to the fate of the first María Islands eddy, the first Cabo Corrientes eddy was reinforced by the more recent CTW via interaction with the new Cabo Corrientes eddy, while the latter was greatly weakened by the exchange (Figures 8r and 8s). The second downwelling CTW also formed a new and stronger María Islands eddy (Figures 8p–8u).

[27] On April 7, 1992 a strong upwelling CTW arrived in the region. The new anticyclonic Cabo Corrientes eddy dies and is replaced by a new cyclonic María Islands eddy generated by the CTW (Figures 8t–8v). The surviving newer anticyclonic and cyclonic eddies detached from the coast and propagated westward (Figures 8s–8z4) along

Figure 8. SSH anomaly (color contours in cm) for 30 different dates in January–May 1992 as determined from Pacific NLOM (experiment PBT7ECH). The positions of Manzanillo (MNZ), Cabo Corrientes (CC), María Islands (MI), Mazatlán (MZT), and Cabo San Lucas (CSL) are indicated. The white line represents the position of the hydrographic transect where the temperature field in Figure 12 was measured in May 1992.

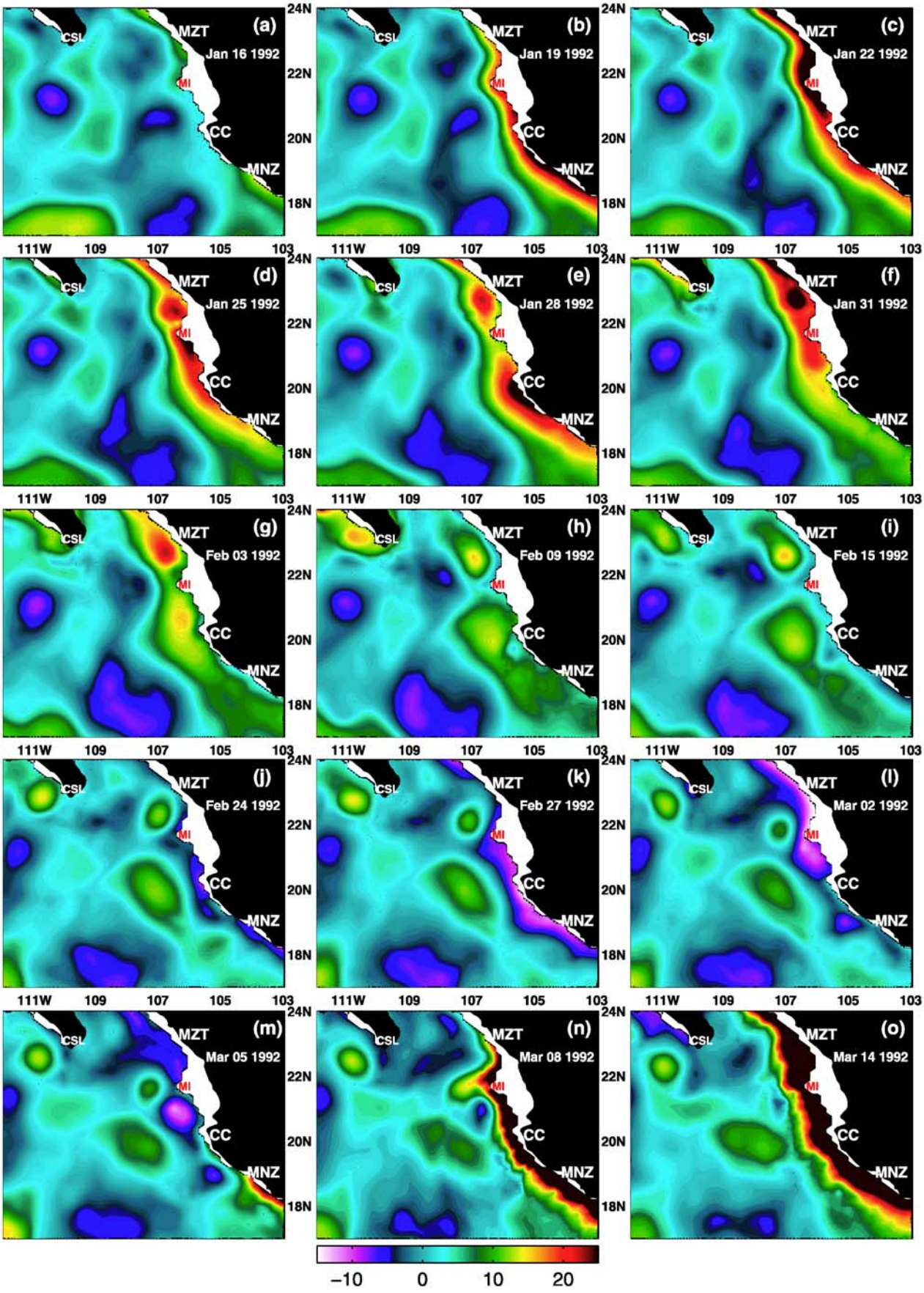
(a) Jan 16 1992
(b) Jan 19 1992
(c) Jan 22 1992
(d) Jan 25 1992
(e) Jan 28 1992
(f) Jan 31 1992
(g) Feb 03 1992
(h) Feb 09 1992
(i) Feb 15 1992
(j) Feb 24 1992
(k) Feb 27 1992
(l) Mar 02 1992
(m) Mar 05 1992
(n) Mar 08 1992
(o) Mar 14 1992
CSL
MZT
MI
CC
MNZ
24N
22N
20N
18N
111W
109
107
105
103
−10
0
10
20

Figure 8

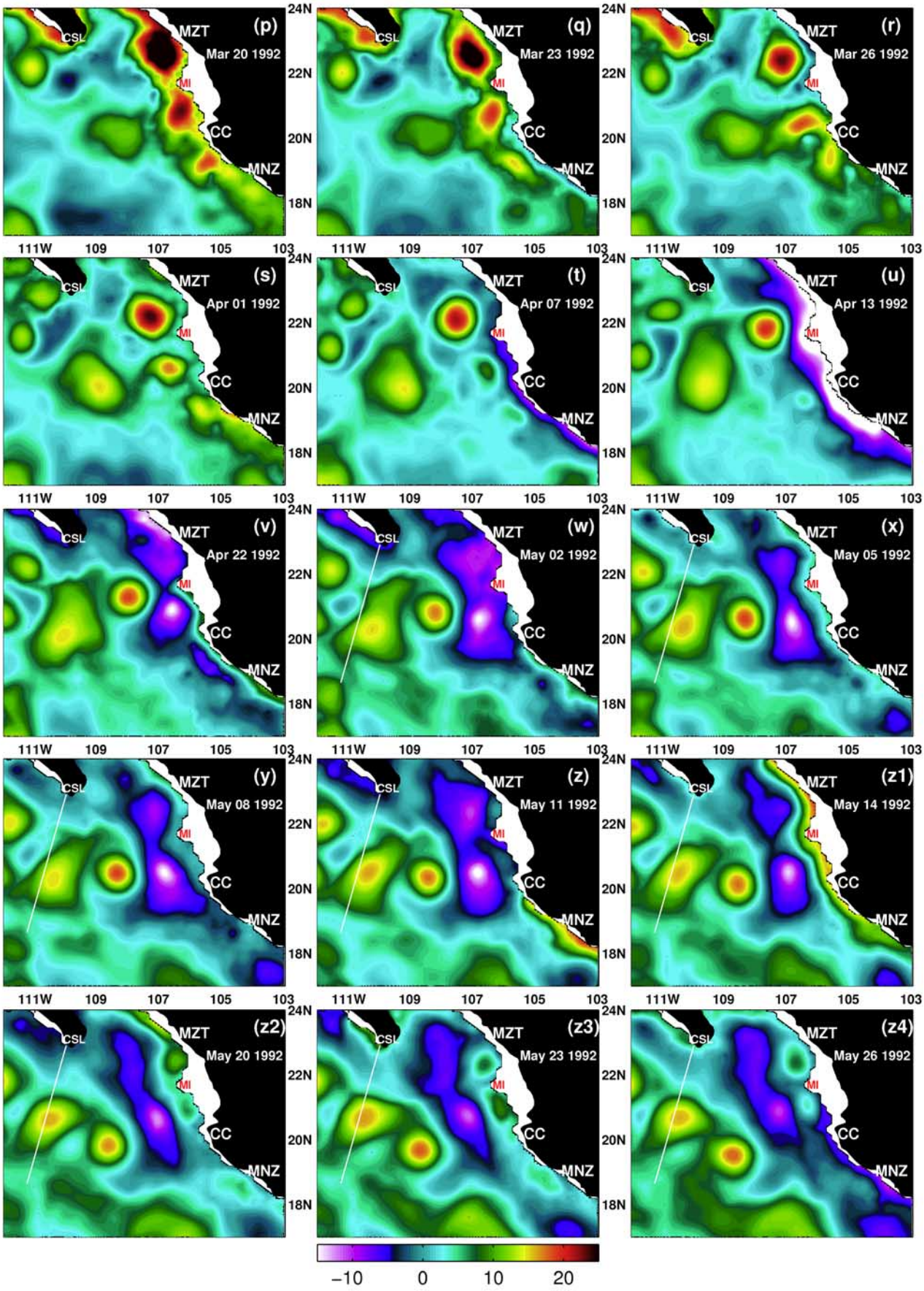

Figure 8. (continued)

Table 2. Number of Anticyclonic Eddies Generated Per Year During the Passage of Coastally Trapped Waves Through the Cabo Corrientes – María Islands Region (Experiment PBT7ECH)

Year	Cabo Corr.	María Is.	Year	Cabo Corr.	María Is.
1979	2	3	1991	3	3
1980	1	1	1992	4	4
1981	2	2	1993	4	3
1982	4	4	1994	2	2
1983	4	5	1995	2	2
1984	1	1	1996	2	3
1985	1	1	1997	5	6
1986	3	3	1998	3	3
1987	4	4	1999	1	1
1988	0	0	2000	1	0
1989	1	1	2001	2	2
1990	2	3	Total	54	57
			Average/year	2.35	2.5

with anticyclonic eddies generated by the first downwelling CTW.

[28] The mesoscale features documented in Figure 8 are some examples that illustrate the key role of CTWs in the formation of the Cabo Corrientes and María Islands eddies. These are not unusual examples. All the simulations forced with 6-hourly winds include the formation of eddies at Cabo Corrientes and the María Islands during the passage of CTWs through the region. The number of eddies formed per year in the 1979–2001 core simulation (experiment PBT7ECH) are summarized in Table 2. In general, those results indicate that on average the CTWs generate 2.35 Cabo Corrientes and 2.5 María Islands anticyclonic eddies per year. The eddies included in that average have similar or larger horizontal and vertical dimensions than those in Figure 8. Some general characteristics of the eddy formation process were found. (1) When the eddies have separated from the coast a distance no farther than ~100 km and a new CTW arrives in the area, the eddy is reinforced and/or fused with a new eddy generated by the latest CTW. Thus, a packet of CTWs arriving in the Cabo Corrientes - María Islands region results in the generation of one large eddy, which is characterized by a radius of ~75 km or more (i.e., Figures 1 and 8t). (2) The formation of eddies varies interannually. During 1988, a La Niña year (Figure 9), no eddies were formed. In contrast, 1997, an El Niño year (Figure 9), was the most prolific year with eleven anticyclonic eddies generated (Table 2). Some of these eddies were characterized by a deeper core than the local currents and the CTW where they originated. (3) El Niño seemed to intensify the eddies. The CTWs associated with the 1982, 1987, 1991 and 1997 El Niño events generated currents >100 cm/s in both the CTWs and the eddies, and the anticyclonic eddies with the largest dimensions. The proliferation (reduction) of large Cabo Corrientes - María Islands eddies during El Niño (La Niña) years is consistent with the results of *Kessler et al.* [1995]. They found an increase (decrease) in the number of Westerly wind events in the western equatorial Pacific during El Niño (La Niña) years. Those wind events are often the generator of baroclinic downwelling Kelvin waves. After crossing the equatorial basin these waves arrive at the Americas west coast and force baroclinic downwelling poleward-propagating CTWs that generate eddies during their passage through the Cabo Corrientes - María Islands region. Furthermore, according to the Japanese Meteorology Agency El Niño Index, 1992 was

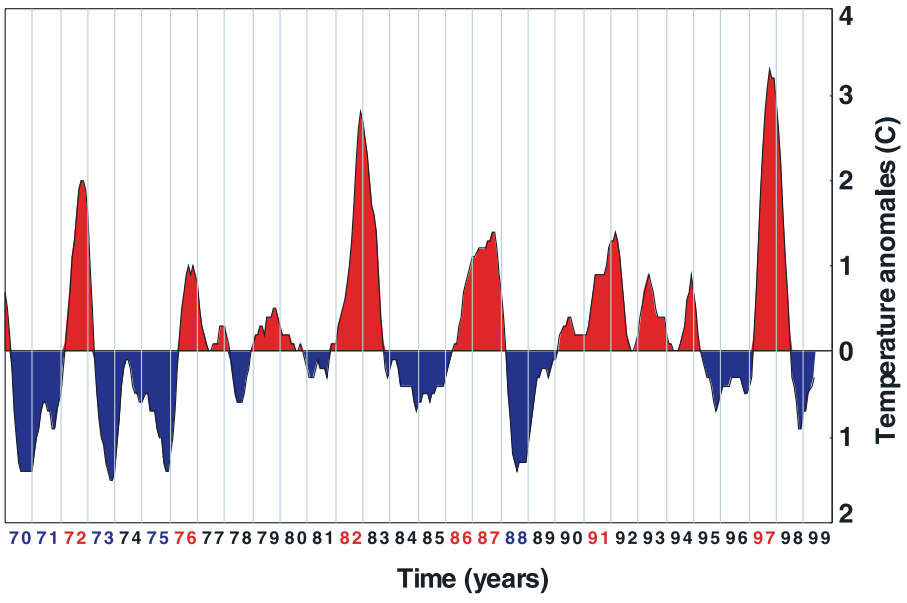

Figure 9. Japanese Meteorological Agency (JMA) El Niño index. Years on the axis in black correspond to neutral events, in blue to La Niña events, and in red to El Niño events. The JMA index defines El Niño (La Niña) events based on sea surface temperature anomalies in the region 4°N–4°S and 150°–90°W. An El Niño (La Niña) event is observed when the 5-month running average of positive (negative) SST anomalies has an amplitude >0.5°C for at least 6 consecutive months. Furthermore, the series of 6 consecutive months must begin before September and must include October, November, and December [*JMA*, 1991; *O'Brien et al.*, 1996].

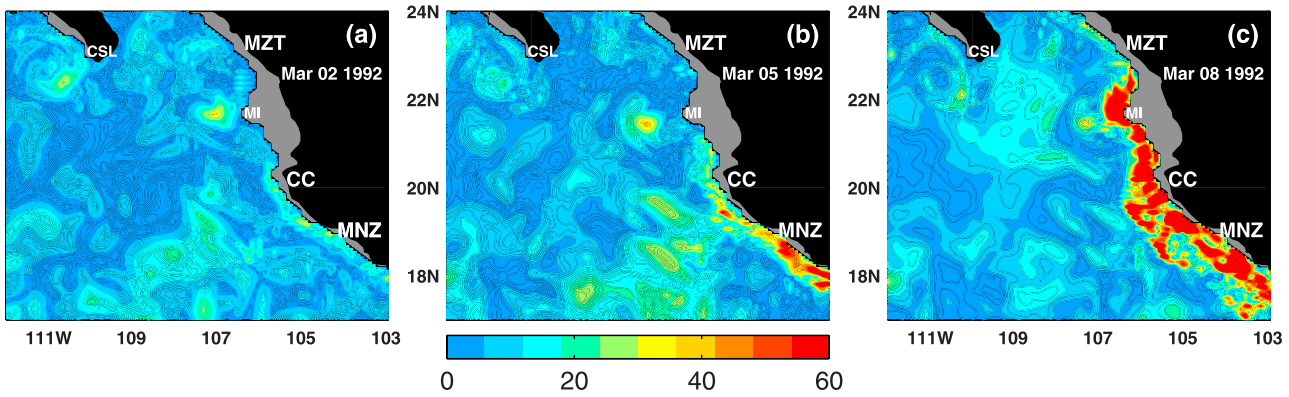

Figure 10. Magnitude of the vectorial velocity difference for three different dates in early March 1992 as determined from Pacific NLOM layer 1 minus layer 2 (color contours in cm/s) (experiment PBT7ECH). The positions of Manzanillo (MNZ), Cabo Corrientes (CC), María Islands (MI), Mazatlán (MZT), and Cabo San Lucas (CSL) are indicated.

classified as a neutral year, but 1991 was classified as El Niño year (Figure 9), but Figure 9 shows the 1991 El Niño event extending into 1992 with a peak in early 1992. This is consistent with the increase in CTWs in the Cabo Corrientes - María Islands region during January–May of 1992 (Figure 8). Consequently, the increase in eddy formation is a result of the increased generation of intraseasonal downwelling equatorial Kelvin waves during the winter of 1991–1992 and the fact that it takes ~2–3 months for the waves to propagate, at ~2.7 m/s, from the central-western equatorial Pacific to the Cabo Corrientes – María Islands region. (4) All downwelling CTWs, which arrived in the Cabo Corrientes – María Islands region generated eddies. In contrast, only some upwelling CTWs generated eddies in this region. This may occur because poleward-propagating upwelling (downwelling) CTWs induce equatorward (poleward) currents, which oppose (strengthen) the poleward local mean currents discussed in section 3.1.

3.2.2. Baroclinic Instabilities, Bottom Topography, and Local Wind

[29] Both the local mean currents in the Cabo Corrientes - María Islands region and the CTWs discussed here are directly or remotely generated by the wind. The arrival of baroclinic downwelling CTWs in the Cabo Corrientes - María Islands region corresponds to the intensification of the locally driven normally poleward surface currents, to the formation of a strong vertical shear in the horizontal currents (Figure 10), and to a sharp drop (rise) of the thermocline (SSH) toward the coast (Figures 8l and 8m), which make them potential candidates for the development of baroclinic instabilities, since baroclinic instabilities occur when perturbations grow by drawing energy from the available potential energy associated with sloping isopycnals [*Kundu*, 1990]. Although ocean currents are constantly exposed to perturbations of different wavelengths, they are predisposed to the propagation and growth of a limited range of wavelengths. The results of the five simulations forced with six-hourly winds include eddy formation associated with the arrival of CTWs in the Cabo Corrientes - María Islands region (Table 1 and Figure 6). Hence, taking into account that the 1.5-layer reduced-gravity simulation (PRG1.5ECH) does not include baroclinic instabilities but does include eddy formation (Figure 6a), we concluded that baroclinic instabilities are not a necessary element in the Cabo Corrientes - María Islands eddy formation.

[30] Bottom topography can have a strong influence on oceanic flow and can influence eddy formation and the detachment of eddies from the coast. The effects of bottom topography were isolated as follows. The 1.5-layer reduced gravity (PRG1.5ECH) and the flat bottom (PFB6ECH) simulations do not include any topographic effect. However, they do include eddy formation at Cabo Corrientes and the María Islands (Figures 6a and 6b), suggesting that the bottom topography can be ruled out as primary factor in the Cabo Corrientes - María Islands' eddy generation. Also, the flat bottom and the reduced-gravity experiments did not include any topographic β effect. However, they include eddy formation and detachment of eddies from the coast, suggesting that the topographic β effect is not a crucial element in the detachment of the Cabo Corrientes and María Islands eddies.

[31] The local wind stress curl is a potential alternative generator of eddies. The wind stress curl snapshots (not shown) corresponding to the example documented in Figure 8 were analyzed. That wind is characterized by a nearshore positive wind stress curl, which could force cyclonic eddies, but not the satellite-measured and model-simulated anticyclonic eddies (Figure 1 and Figures 6–8). Also, both the wind stress curl snapshots and the means in Figure 3 are mostly characterized by a weak upwelling favorable wind that would oppose the local mean poleward currents and the poleward currents associated with the passage of downwelling CTWs but reinforce the equatorward currents associated with the passage of upwelling CTWs. Then, in summary, the evidence suggests that the local wind did not force or substantially contribute to the development of the anticyclonic Cabo Corrientes – María Islands eddies.

[32] In summary, factors discussed in this subsection may influence the formation and evolution of eddies in the Cabo Corrientes/María Islands region, but none of them are crucial to their existence, including their development and detachment from the coast. The capes, the strong transient currents generated by the CTWs and nondispersive westward propagation are crucial to their development and separation from the coast.

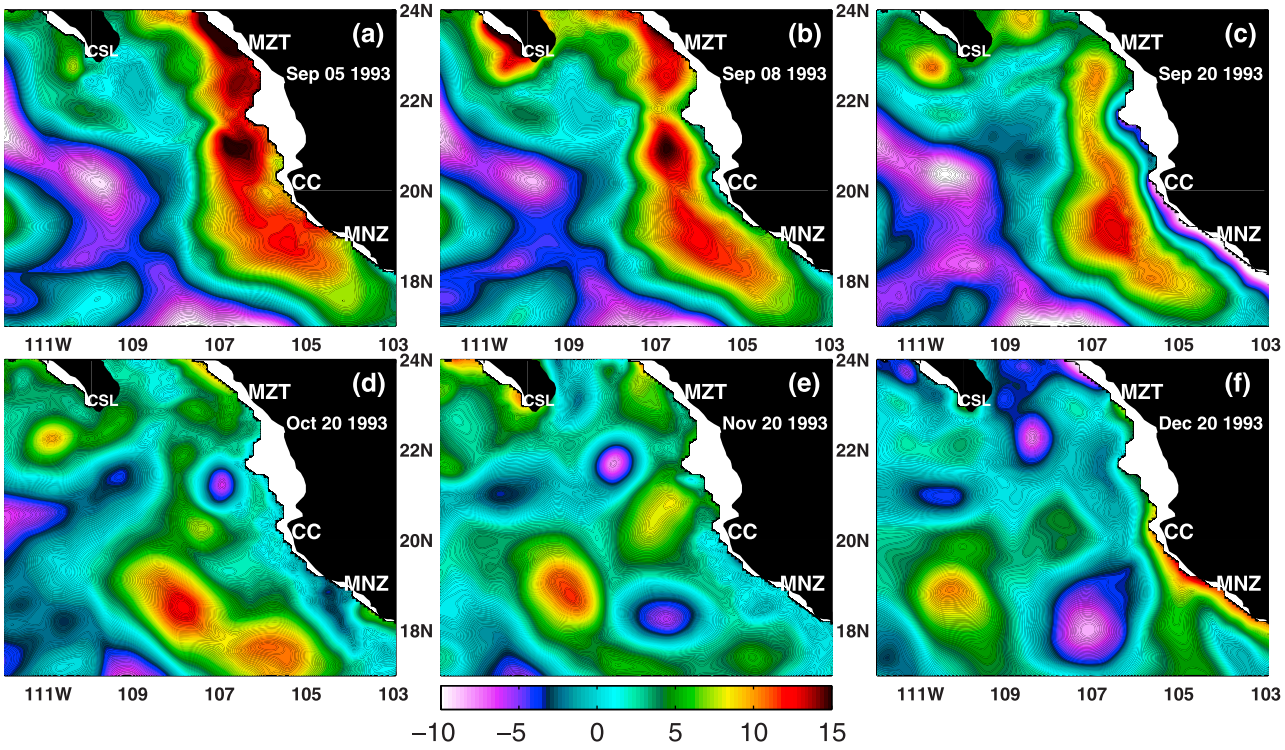

Figure 11. SSH anomaly (color contours in cm) for six different dates in September–December 1993 as determined from Pacific NLOM (exp. PBT7ECH). The positions of Manzanillo (MNZ), Cabo Corrientes (CC), María Islands (MI), Mazatlán (MZT), and Cabo San Lucas (CSL) are indicated.

3.2.3. Observed and Modeled Eddies

[33] The model results show anticyclonic eddy formation each time a CTW arrives in the Cabo Corrientes – María Islands region. If our eddy-generation hypothesis is correct, we would expect to observe anticyclonic eddies close to Cabo Corrientes and the María Islands in TOPEX/ERS satellite-altimeter measurements. Examination of altimeter SSH measurements during September–December 1993 reveals the presence and west-southwestward propagation of an anticyclonic eddy near Cabo Corrientes (Figure 1). Correspondingly, the simulated SSH shows that in early September 1993 a baroclinic downwelling CTW arrived in the Cabo Corrientes - María Islands region, generating an anticyclonic eddy close to Cabo Corrientes (Figure 11). That eddy was characterized by a maximum SSH anomaly of ∼15 cm during its early stages (Figures 11a and 11b). After its generation and detachment from the coast, the eddy propagated southwestward (Figures 11c–11f). By December 20, 1993 the eddy was located close to 110°W, 19°N, and it was characterized by maximum SSH anomaly, radius, and swirl velocity of ∼10 cm, ∼60 km, and ∼50 cm/s, respectively. A qualitative comparison between the measured and simulated SSH indicates that the model reproduces the measured SSH anomaly of ∼15 cm, during the eddy formation and detachment (Figures 1 and 11). However, during the three month time frame shown in Figures 1 and 11, the simulated eddy decayed and drifted southward more rapidly than the measured one. For instance, on November 20, 1993 the center of the measured eddy was located close to 109°W, 20.5°N, while the center of the simulated eddy was located close to 109°W, 19°N (Figures 1c and 11c). Also, the SSH maximum of the measured (∼15 cm) and simulated (∼12 cm) eddy differs by ∼3 cm on this date. In spite of these differences, Figures 1 and 11 show that the simulated and measured eddy have similar spatial features and they are approximately co-located, in time and space, suggesting that the satellite-altimeter measured eddy was generated by the CTW that arrived in the Cabo Corrientes – María Islands region in early September 1993 (Figure 11). It is important to mention that the example in Figure 1 is not an unusual event. In fact, several other examples of eddy formation near Cabo Corrientes and the María Islands have been observed using the Colorado Center for Astrodynamics Research publicly accessible web site (http://www-ccar.colorado.edu/∼realtime/global-historical_ssh).

[34] To provide some insight into the validation of the Cabo Corrientes – María Islands eddy generation hypothesis, we compared model results with hydrographic data. Using hydrographic temperature data, *Trasviña et al.* [1999] reported transversal sections of temperature versus depth which show a downward bending of the isoterms that reach a maximum depth between 20°N and 21°N, suggesting the presence of an anticyclonic eddy located ∼500 km to the west of Cabo Corrientes (Figure 12). The model results in Figure 8 suggest that the eddy measured by *Trasviña et al.* [1999] was not generated near the location of observation. In fact, the results suggest that the eddy was created in early February 1992 on the north side of Cabo Corrientes as a result of CTW passage through the area (Figures 8a–8f). Next, the eddy was influenced by the strong CTW that passed by the capes in early March 1992 (Figures 8m–8o). Later, the eddy drifted westward (Figures 8p–8z4), passing through the line where the hydrographic data were taken in

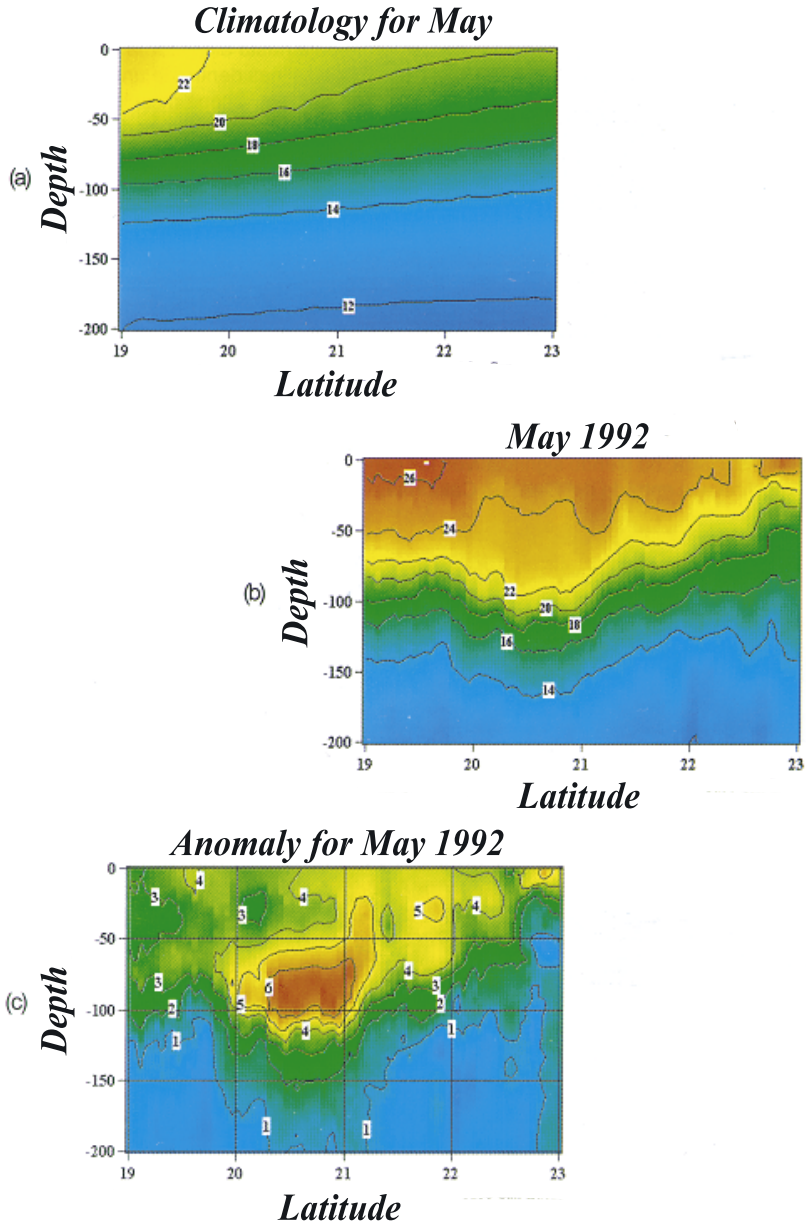

Figure 12. Latitude-depth sections of temperature (in °C) along the white line in Figure 8. (a) Climatological mean temperature for May. (b) Monthly mean temperature for May 1992. (c) Temperature anomaly for May 1992. Adapted from *Trasviña et al.* [1999].

May 1992 (Figures 8w–8z4), and where a positive subsurface temperature anomaly was observed (Figure 12c).

4. Summary and Concluding Remarks

[35] The existence of the Cabo Corrientes and María Islands eddies is being reported for the first time. The eddy generation processes are investigated using a suite of high-resolution (1/16°) numerical simulations from the Naval Research Laboratory (NRL) Layered Ocean Model (NLOM). The model results show the existence of mean poleward coastal currents that extend from ~17°N to the entrance of the Gulf of California and originate as the ocean response to the local wind forcing. These local currents do not generate eddies in the Cabo Corrientes - María Islands region by themselves. Eddies are generated when coastally trapped waves, which are forced by Equatorial Pacific Kelvin Waves, arrive in the Cabo Corrientes - María Islands region and intensify the local currents. The intensified-currents are perturbed by the Cabo Corrientes and María Islands capes and separate from the coast. Both, the local currents and the currents associated with the coastally trapped waves have a coastally trapped nature. After separation from the coast on the downstream side of the capes, the intensified-currents reattach to the coast farther downstream. The separation and reattachment produce distinctive anticyclonic closed circulations, which evolve into the Cabo Corrientes and María Islands eddies that propagate away from the coast after the CTW have exited the area. On average, from 1979 to 2001, the coastally trapped waves

generate 2.35 Cabo Corrientes and 2.5 María Islands anticyclonic eddies per year in the model. Also, the generation of Cabo Corrientes and María Islands eddies varies interannually, increasing (decreasing) during El Niño (La Niña) years. Those eddies are characterized by an average sea surface high anomaly, radius, and swirl velocity of ~15 cm, ~50 km, and 45 cm/s, respectively. The ability of the numerical simulations to isolate the dynamic effects allows us to rule out the local wind, bottom topography, and baroclinic instabilities as necessary factors in the eddy generation processes. Validation of the eddy generation hypothesis, and the model simulated eddies is based on the qualitative comparison of the model results with hydrographic temperature data, and with TOPEX/Poseidon and ERS-2 satellite altimeter sea surface height measurements.

[36] Finally from the results of this research a corollary is derived: Intraseasonal coastally trapped waves do not excite a westward radiation of energy in the form of non dispersive internal Rossby waves [*Enfield*, 1987; *Clarke and Shi*, 1991]. However, the examples in Figures 8 and 11 show that intraseasonal coastally trapped waves generate eddies, at Cabo Corrientes and the María Islands, which do propagate west-southwestward as isolated nonlinear eddies.

[37] **Acknowledgments.** This is a contribution to the 6.1 project Global Remote Littoral Forcing via Deep Water Pathways funded by the Office of Naval Research (ONR) under program element 601153N. The numerical simulations were performed on Cray T3E computers at the Naval Oceanographic Office, Stennis Space Center, Mississippi, and the Engineering Research and Development Center, Vicksburg, Mississippi, using grants on computer time provided by the Department of Defense High Performance Computing Modernization Program. L.Z. was funded by the 6.2 project Coastal Ocean Nesting Studies during the last part of this research. This paper is NRL contribution NRL/JA/7304/04/0001.

References

Badan-Dangon, A. (1998), Coastal circulation from the Galápagos to the Gulf of California, in *The SEA, The Global Coastal Ocean, Regional Studies and Syntheses*, vol. 11, edited by A. R. Robinson and K. H. Brink, pp. 315–343, John Wiley, New York.

Badan-Dangon, A., J. M. Robles and J. García (1989), Poleward flows off Mexico's Pacific coast, in *Poleward Flows Along Eastern Ocean Boundaries*, edited by S. J. Neshyba, C. N. K. Mooers, R. L. Smith, and R. T. Barber, pp. 176–201, Springer, New York.

Bormans, M., and C. Garret (1989), A simple criterion for gyre formation by the surface outflow from a strait, with application to the Alboran Sea, *J. Geophys. Res.*, *94*, 12,637–12,644.

Cenedese, C., and J. A. Whitehead (2000), Eddy shedding from a boundary current around a cape over a sloping bottom, *J. Phys. Oceanogr.*, *30*, 1514–1531.

Chelton, D. B., and R. E. Davis (1982), Monthly mean sea level variability along the west coast of North America, *J. Phys. Oceanogr.*, *12*, 757–784.

Christensen, N., Jr., R. de la Paz, and G. Gutierrez (1983), A study of sub-inertial waves off the west coast of Mexico, *Deep Sea Res.*, *30*, 835–850.

Clarke, A. J., and C. Shi (1991), Critical frequencies at ocean boundaries, *J. Geophys. Res.*, *96*, 10,731–10,738.

Crawford, W. R., J. Y. Cherniawsky, M. G. G. Foreman, and J. F. R. Gower (2002), Formation of the Haida-1998 oceanic eddy, *J. Geophys. Res.*, *107*(C7), 3069, doi:10.1029/2001JC000876.

D'Asaro, E. (1988), Generation of submesoscale vortices: A new mechanism, *J. Geophys. Res.*, *93*, 6685–6694.

Di Lorenzo, E., M. G. G. Foreman, and W. R. Crawford (2005), Modeling the generation of Haida eddies, *Deep Sea Res., Part II*, *52*(7-8), 853–874.

Enfield, D. B. (1987), The intraseasonal oscillation in Eastern Pacific sea levels: How is it forced?, *J. Phys. Oceanogr.*, *17*, 1860–1876.

Enfield, D. B., and J. S. Allen (1983), The generation and propagation of sea level variability along the Pacific coast of Mexico, *J. Phys. Oceanogr.*, *13*, 1012–1033.

European Centre for Medium-Range Weather Forecasts (ECMWF) (1994), The description of the ECMWF/WCRP level III—A global atmospheric data archive, report, 72 pp., Reading, UK.

Hellerman, S., and M. Rosenstein (1983), Normal monthly wind stress over the world ocean with error estimates, *J. Phys. Oceanogr.*, *13*, 1093–1104.

Hogan, P. J., and H. E. Hurlburt (2000), Impact of upper ocean – topographic coupling and isopycnal outcropping in Japan/East Sea models with 1/8° to 1/64° resolution, *J. Phys. Oceanogr.*, *30*, 2535–2561.

Hogan, P. J., and H. E. Hurlburt (2005), Sensitivity of simulated circulation dynamics to the choice of surface wind forcing in the Japan/East Sea, *Deep Sea Res., Part II*, *52*, 1464–1489.

Hughes, R. L. (1989), The hydraulics of local separation in a coastal current with application to the Kuroshio Meander, *J. Phys. Oceanogr.*, *19*, 1809–1820.

Hurlburt, H. E., and P. J. Hogan (2000), Impact of 1/8° to 1/64° resolution on Gulf Stream model-data comparisons in basin-scale subtropical Atlantic Ocean models, *Dyn. Atmos. Ocean*, *32*, 283–329.

Hurlburt, H. E., and E. J. Metzger (1998), Bifurcation of the Kuroshio Extension at the Shatsky Rise, *J. Geophys. Res.*, *103*, 7549–7566.

Hurlburt, H. E., and J. D. Thompson (1980), A numerical study of Loop Current intrusions and eddy-shedding, *J. Phys. Oceanogr.*, *10*, 1611–1651.

Hurlburt, H. E., P. J. Hogan, E. J. Metzger, W. J. Schmitz Jr., and A. J. Wallcraft (1996), Dynamics of the Kuroshio/Oyashio current system using eddy-resolving models of the North Pacific Ocean, *J. Geophys. Res.*, *101*, 941–976.

Japanese Meteorological Agency (JMA) (1991), Climate charts of sea surface temperatures of the western North Pacific and the Global Ocean, 51 pp., Mar. Div., Tokyo.

Kara, A. B., P. A. Rochford, and H. E. Hurlburt (2002), Air-sea flux estimates and the 1997–1998 ENSO event, *Boundary Layer Meteorol.*, *103*, 439–458.

Kara, A. B., H. E. Hurlburt, P. A. Rochford, and J. J. O'Brien (2004), The impact of water turbidity on interannual sea surface temperature simulations in a layered global ocean model, *J. Phys. Oceanogr.*, *34*, 345–359.

Kessler, W. S. (2002), Mean three-dimensional circulation in the northeast tropical Pacific, *J. Phys. Oceanogr.*, *32*, 2457–2471.

Kessler, W. S., M. J. McPhaden, and K. M. Weickmann (1995), Forcing of intraseasonal Kelvin waves in the equatorial Pacific, *J. Geophys. Res.*, *100*, 10,613–10,631.

Klinger, B. (1994a), Baroclinic eddy generation at a sharp corner in a rotating system, *J. Geophys. Res.*, *99*, 12,515–12,531.

Klinger, B. (1994b), Inviscid current separation from rounded capes, *J. Phys. Oceanogr.*, *24*, 1805–1811.

Kundu, P. K. (1990), *Fluid Mechanics*, 638 pp., Academic, San Diego, Calif.

Levitus, S., and T. P. Boyer (1994), World Ocean Atlas 1994, vol. 4, Temperature, NOAA Atlas NESDIS, 117 pp., Natl. Oceanic and Atmos. Admin., Silver Spring, Md.

Levitus, S., R. Burgett, and T. P. Boyer (1994), World Ocean Atlas 1994, vol. 3, Salinity, NOAA Atlas NESDIS, 99 pp., Natl. Oceanic and Atmos. Admin., Silver Spring, Md.

López, M., L. Zamudio, and F. Padilla (2005), Effects of the 1997–1998 El Niño on the exchange of the northern Gulf of California, *J. Geophys. Res.*, *110*, C11005, doi:10.1029/2004JC002700.

Melsom, A., S. D. Meyers, H. E. Hurlburt, E. J. Metzger, and J. J. O'Brien (1999), ENSO effects on Gulf of Alaska eddies, *Earth Interactions*, *3*(1), 1–30. (Available at http://www.EarthInteractions.org)

Melsom, A., E. J. Metzger, and H. E. Hurlburt (2003), Impact of remote oceanic forcing on Gulf of Alaska sea levels and mesoscale circulation, *J. Geophys. Res.*, *108*(C11), 3346, doi:10.1029/2002JC001742.

Merrifield, M. A. (1992), A comparison of long coastal-trapped wave theory with remote-storm-generated wave events in the Gulf of California, *J. Phys. Oceanogr.*, *22*, 5–18.

Merrifield, M. A., and C. D. Winant (1989), Shelf circulation in the Gulf of California: A description of the variability, *J. Geophys. Res.*, *94*, 18,133–18,160.

Metzger, E. J., and H. E. Hurlburt (1996), Coupled dynamics of the South China Sea, the Sulu Sea, and the Pacific Ocean, *J. Geophys. Res.*, *101*, 12,331–12,352.

Metzger, E. J., and H. E. Hurlburt (2001), The nondeterministic nature of Kuroshio penetration and eddy shedding in the South China Sea, *J. Phys. Oceanogr.*, *31*, 1712–1732.

Metzger, E. J., H. E. Hurlburt, J. C. Kindle, Z. Sirkes, and J. M. Pringle (1992), Hindcasting wind-driven anomalies using a reduced gravity global ocean model, *J. Mar. Technol. Soc.*, *26*(2), 23–32.

Meyers, S. D., A. Melsom, G. T. Mitchum, and J. J. O'Brien (1998), Detection of fast Kelvin wave teleconnection due to El Niño–Southern Oscillation, *J. Geophys. Res.*, *103*, 27,665–27,663.

Moore, D. R., and A. J. Wallcraft (1998), Formulation of the NRL Layered Ocean Model in spherical coordinates, *Nav. Res. Lab. Rep. NRL/CR/7323-96-0005*, 24 pp., Stennis Space Cent., Miss.

Murray, C. P., S. L. Morey, and J. J. O'Brien (2001), Interannual variability of upper ocean vorticity balances in the Gulf of Alaska, *J. Geophys. Res.*, *106*, 4479–4491.

National Oceanic and Atmospheric Administration (NOAA) (1986), ETOPO5 digital relief of the surface of the earth, *Data Announce. 86-MGG-07*, Natl. Geophys. Data Cent., Washington, D. C.

O'Brien, J. J., T. S. Richards, and A. C. Davis (1996), The effect of El Niño on U.S. landfalling hurricanes, *Bull. Am. Meteorol. Soc.*, *77*, 773–774.

Pichevin, T., and D. Nof (1996), The eddy cannon, *Deep Sea Res.*, *43*, 1475–1507.

Ramp, S. R., J. L. McClean, C. A. Collins, A. J. Semtner, and K. A. S. Hays (1997), Observations and modeling of the 1991–1992 El Niño signal off central California, *J. Geophys. Res.*, *102*, 5553–5582.

Rhodes, R. C., et al. (2002), Navy real-time global modeling systems, *Oceanography*, *15*(1), 30–44.

Røed, L. P. (1980), Curvature effects on hydraulically driven inertial boundary currents, *J. Fluid Mech.*, *90*, 395–412.

Rosmond, T. E., J. Teixeira, M. Peng, T. F. Hogan, and R. Pauley (2002), Navy Operational Global Atmospheric Prediction System (NOGAPS): Forcing for ocean models, *Oceanography*, *15*(1), 99–108.

Shriver, J. F., and H. E. Hurlburt (1997), The contribution of the global thermohaline circulation to the Pacific to Indian Ocean throughflow via Indonesia, *J. Geophys. Res.*, *102*, 5491–5511.

Shriver, J. F., H. E. Hurlburt, O. M. Smedstad, A. J. Wallcraft, and R. C. Rhodes (2007), 1/32° real-time global ocean prediction and value-added over the 1/16° resolution, *J. Mar. Syst.*, *65*, 3–26.

Smedstad, O. M., H. E. Hurlburt, E. J. Metzger, R. C. Rhodes, J. F. Shriver, A. J. Wallcraft, and A. B. Kara (2003), An operational Eddy resolving 1/16° global ocean nowcast/forecast system, *J. Mar. Syst.*, *40-41*, 341–361.

Smith, D. C., IV, and A. A. Bird (1989), Factors influencing asymmetry and self advection in ocean eddies, in *The 20th Annual Symposium on Ocean Hydrodynamics, Elsevier Oceanogr. Ser.*, edited by J. C. J. Nihoul, pp. 211–225, Elsevier, New York.

Spillane, M. C., D. B. Enfield, and J. S. Allen (1987), Intraseasonal oscillations in sea level along the west coast of the Americas, *J. Phys. Oceanogr.*, *17*, 313–325.

Strub, P. T., P. M. Kosro, and A. Huyer (1991), The nature of the cold filaments in the California Current system, *J. Geophys. Res.*, *96*, 14,743–14,768.

Sverdrup, H. U. (1947), Wind-driven currents in a baroclinic ocean; with application to the equatorial currents of the eastern Pacific, *Proc. Natl. Acad. Sci.*, *33*, 318–326.

Tilburg, C. E., H. E. Hurlburt, J. J. O'Brien, and J. F. Shriver (2001), The dynamics of the East Australian Current system: the Tasman Front, the East Auckland Current, and the East Cape Current, *J. Phys. Oceanogr.*, *31*, 2917–2943.

Tilburg, C. E., H. E. Hurlburt, J. J. O'Brien, and J. F. Shriver (2002), Remote topographic forcing of a baroclinic western boundary current: An explanation for the southland current and the pathway of the subtropical front east of New Zealand, *J. Phys. Oceanogr.*, *32*, 3216–3232.

Trasviña, A., D. L. Cota, A. E. Filonov, and A. Gallegos (1999), Oceanografía y El Niño, in *Los Impactos de El Niño en México*, edited by V. O. Magaña, pp. 69–101, Univ. Nac. Autón. de México, México.

Wallcraft, A. J. (1991), The Navy Layered Ocean Model users guide, *NOARL Rep. 35*, 21 pp., Nav. Res. Lab., Stennis Space Cent., Miss.

Wallcraft, A. J., and D. R. Moore (1997), The NRL Layered Ocean Model, *Parallel Comput.*, *23*, 2227–2242.

Wallcraft, A. J., A. B. Kara, H. E. Hurlburt, and P. A. Rochford (2003), The NRL Layered Ocean Model (NLOM) with an embedded mixed layer submodel: Formulation and tuning, *J. Atmos. Oceanic Technol.*, *20*, 1601–1615.

Zamudio, L., A. P. Leonardi, S. D. Meyers, and J. J. O'Brien (2001), ENSO and eddies on the southwest coast of Mexico, *Geophys. Res. Lett.*, *28*(1), 13–16.

Zamudio, L., H. E. Hurlburt, E. J. Metzger, and O. M. Smedstad (2002), On the evolution of coastally trapped waves generated by Hurricane Juliette along the Mexican west coast, *Geophys. Res. Lett.*, *29*(23), 2141, doi:10.1029/2002GL014769.

Zamudio, L., H. E. Hurlburt, E. J. Metzger, S. L. Morey, J. J. O'Brien, C. Tilburg, and J. Zavala-Hidalgo (2006), Interannual variability of Tehuantepec eddies, *J. Geophys. Res.*, *111*, C05001, doi:10.1029/2005JC003182.

H. E. Hurlburt and E. J. Metzger, Naval Research Laboratory, Stennis Space Center, MS 39529-5004, USA.

C. E. Tilburg, Department of Chemistry and Physics, University of New England, Biddeford, ME 00405, USA.

L. Zamudio, Center for Ocean-Atmospheric Prediction Studies, Florida State University, Tallahassee, FL 32306-2840, USA. (luis.zamudio@nrlssc.navy.mil)